
The Interpretation of Hard and Soft X-rays from Solar Flares

J. C. Brown

Phil. Trans. R. Soc. Lond. A 1976 **281**, 473-490

doi: 10.1098/rsta.1976.0044

Email alerting service

Receive free email alerts when new articles cite this article - sign up in the box at the top right-hand corner of the article or click [here](#)

The interpretation of hard and soft X-rays from solar flares

BY J. C. BROWN

Department of Astronomy, University of Glasgow, Glasgow, G12 8QQ

The present status of observations of hard X-ray bursts is reviewed in terms of the light they shed on alternative source models and on general characteristics of electron acceleration in flares. Special attention is given to the requirements of total energy release, and the time scale of its release, into energetic electrons on the basis of the normal bremsstrahlung interpretation of bursts. It is particularly emphasized that, since these electrons may dominate the energy balance in many flares, they provide on the one hand an attractive heating mechanism for the thermal flare but, on the other, put severe demands on acceleration mechanisms. A reassessment of the relative merits of synchrotron and inverse Compton source mechanisms is suggested, along with other possibilities, as an escape from this apparent difficulty.

Observational characteristics of soft X-ray flares are cursorily reviewed. The importance of a non-isothermal approach to the physics of the soft X-ray plasma is then illustrated in terms of flare energy flow. It is argued however, that high spectral resolution is not the key to this problem since ill conditioning of the problem prevents useful inference of temperature structure. Instead high resolution imaging with moderate spectral resolution is advocated.

1. INTRODUCTION

Flare research has, like many long-standing fields of astronomy, always been somewhat beset by matters of terminology. Thus, for instance, Švestka has at this meeting suggested that energetic electron production is not the ‘primary’ process in any flare since it is preceded (in time) by a soft X-ray enhancement and since some X-ray bursts have a non-impulsive profile. Though such considerations may be important diagnostics, it seems appropriate to regard the ‘primary’ effect of flares as that involving the greatest energy release rate, rather than to consider morphology or temporal sequence, since this release rate has always been the key problem in flare theory (see, for example, Sweet 1969). In this review, the standpoint adopted is to examine the requirements of flare energy release posed by the X-ray observations. Most of the paper is concerned with hard X-rays ($\gtrsim 10$ keV) and their interpretation in terms of particle acceleration. In the final section (§6) the importance of the soft X-ray plasma in terms of flare energy flow is discussed and it is argued that non-isothermal models are essential in this context. It is shown, however, that due to ill-conditioning of the problem this temperature structure cannot be accurately inferred from soft X-ray spectra, no matter how high the spectral resolution.

For a recent review of satellite-, rocket- and balloon-borne hard X-ray instrumentation the reader is referred to Kane (1974). In the five years or so since the last R. S. Discussion Meeting (in 1970) on the current topic, no radically new hard X-ray data have been obtained. By that time the first detection of polarization (Tindo, Ivanov, Mandelshtam & Shuryghin 1970) and the one and only crude spatial resolution by collimators (Takakura *et al.* 1971) had been achieved. The principal advances have been the acquisition of a large sample of small burst observations (Kane 1974, Datlowe, Elcan & Hudson 1974*a*) for statistical studies; and the

development, for large bursts, of detectors of high time resolution and having well calibrated spectral response, free from pulse pile-up and other problems (e.g. van Beek 1973). Some progress has also been made in the detection and measurement of polarization (Tindo, Ivanov, Mandelshtam & Shuryghin 1972*a*; Tindo, Ivanov, Valnicek & Livshits 1972*b*; Tindo, Mandelshtam & Shuryghin 1973; Nakada, Thomas & Neupert 1974). Reviews of aspects of this observational material and its interpretation have been recently presented by Hudson (1973), Kane (1974), Brown (1975) and Datlowe (1975) among others. The next major step in instrumentation, and hence in observational progress with the problems discussed here, will undoubtedly be the launching of a high resolution hard X-ray heliograph, hopefully in conjunction with improved polarimetry.

2. MODELS OF HARD X-RAY BURST EMISSION

Figure 1 shows schematically the relationship of the hard X-ray burst to other flare emissions (after Kane 1974), namely an impulsive phenomenon synchronous with other flash phase features.

It is now widely presumed that hard X-rays above 10 keV or so are generated by electron-ion collisional bremsstrahlung in the flare plasma by a non-thermal electron component, with a near power-law spectrum, in the same energy range as the emitted photons. This assumed supremacy of the bremsstrahlung mechanism has been essentially based on the analysis by

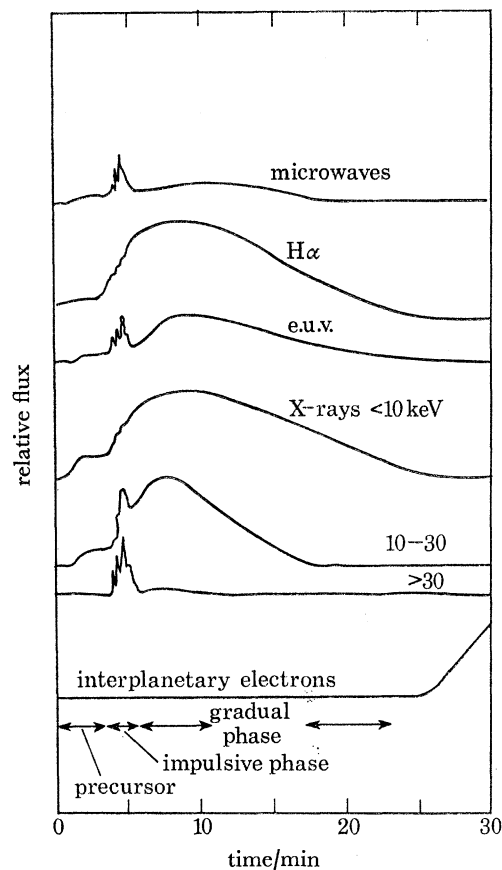


FIGURE 1. Schematic time profile of a solar flare at a variety of wavelengths, according to Kane (1974).

Korchak (1967, 1971) of possible rivals – synchrotron and inverse Compton emission by highly relativistic electrons – though Korchak himself emphasizes the need to take account of these. In this section the main forms of pure bremsstrahlung models in the current literature are discussed. However, in view of the severe demands these make of energy supply in the flare (see §4), some reappraisal is made in §5 of the inverse Compton and synchrotron contributions together with a discussion of the thermal contribution at high energies. It must also be emphasized that no hard X-ray source model to date has incorporated any adequate evaluation of the role which might be played by collective plasma effects in the bremsstrahlung target (cf. Brown 1975).

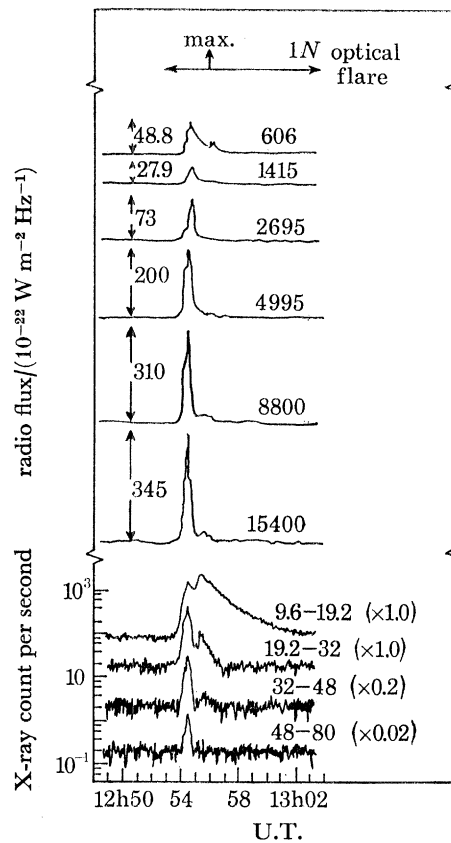


FIGURE 2. Time development of hard X-rays and associated emissions in the small event of 24 May 1968 (Kane 1974). The numbers to the right of the radio profiles indicate the frequency in MHz, and those beside the X-ray profiles the energy bands in keV, the factor in parenthesis being the count rate scaling factor.

Figures 2, 3 and 4 show typical time profiles for, respectively, a small, a moderate and a very large event, at several photon energies. These time profiles have been variously interpreted in terms of schematic models of which the three principal types extant in the literature are shown in figure 5. In both the thick target model – figure 5*a* – (Arnoldy, Kane & Winckler 1968; Brown 1971, 1972*a*, Syrovatskii & Shmeleva 1972; McKenzie, Datlowe & Peterson 1973; Petrosian 1973) and the thin target model – figure 5*b* – (Datlowe & Lin 1973, Lin 1974), the electrons are produced continuously and injected either downward to the dense chromosphere (thick) or upward through the tenuous corona (thin). In both cases the X-ray flux observed ($I(e, t)$ photons $\text{cm}^{-2} \text{s}^{-1} \text{keV}^{-1}$) has a time profile following that of the electron production rate

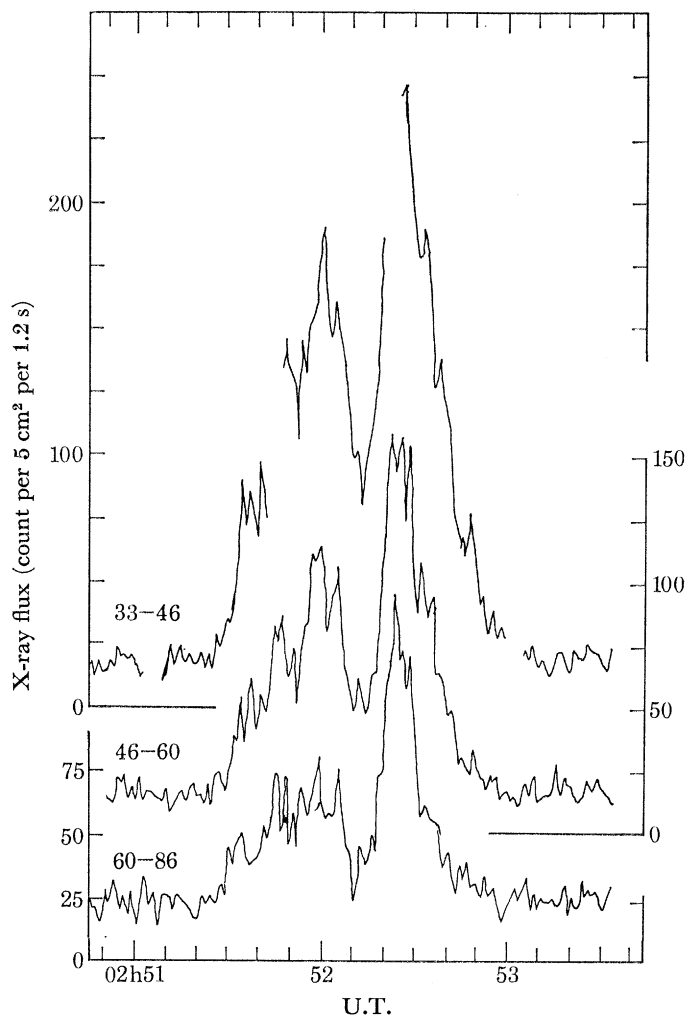


FIGURE 3. Time development of hard X-rays in the moderately large event of 7 August 1972 (Hoyng *et al.* 1975). The numbers on the profiles are energy bands in keV.

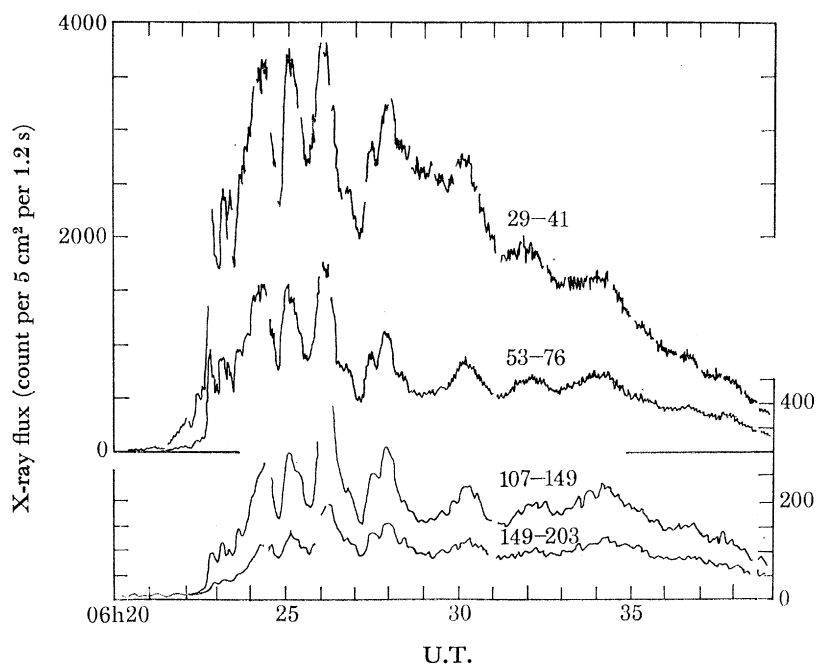


FIGURE 4. Hard X-ray time profile for the very large event of 4 August 1972 (Hoyng *et al.* 1975). Details as for figure 3.

$\mathcal{F}(E, t)$ (electrons $\text{s}^{-1} \text{keV}^{-1}$) but in neither is any physical model of this production rate incorporated since the appropriate time-dependent acceleration problem is still far from solution (cf. review by Smith 1974, for example). Rather the models are used to infer \mathcal{F} from the burst (Brown 1971, 1975). For the usual approximation of $I(e, t)$ to a power-law in energy (cf. §4), i.e.

$$I(e, t) = A(t) e^{-\gamma(t)} \quad (1)$$

the results are

$$\mathcal{F}(E, t) = \frac{6.7 \times 10^{50}}{\Delta N} f(\gamma) A E_0^{-\gamma+1} \quad (2)$$

for a thin target of slab thickness ΔN protons cm^{-2} ($\Delta N \lesssim 10^{19}$) and

$$\mathcal{F}(E, t) = 2.0 \times 10^{33} f(\gamma) A E^{-\gamma-1} \quad (3)$$

for the thick target, with $f(\gamma) = (\gamma - 1)^2 B(\gamma - \frac{1}{2}, \frac{1}{2})$. (In a thick target with purely collisional losses, $\Delta N \rightarrow \infty$, collisional losses are total and the result is independent of density.)

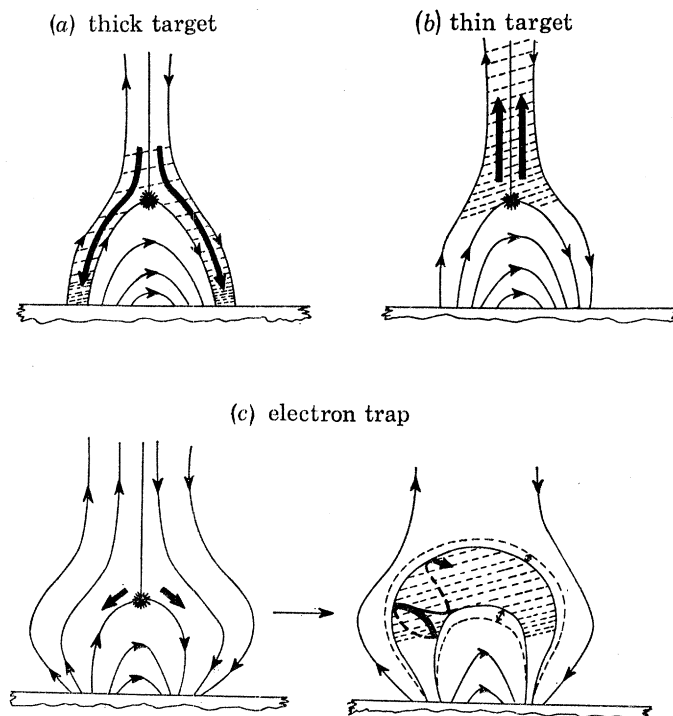


FIGURE 5. Alternative bremsstrahlung models of hard X-ray burst sources. The heavy arrows are schematic of electron paths in each model, emanating from the primary acceleration region (*) and producing bremsstrahlung X-rays with spatial distribution suggested by the dashed line shading. The electron trap model (c) invokes two phases: very rapid injection of electrons (left) followed by coronal trapping modulated by oscillations of the bottle (right) as indicated by dotted flux tube.

According to the third source model – the electron trap model in figure 5c (Takakura & Kai 1966, Takakura 1972, Brown 1972*b*, 1973*a*, Brown & Hoyng 1975) – fast electrons originate in an initial phase of rapid acceleration ('impulsive injection') and are subsequently trapped in a coronal magnetic bottle. The original static version of this model (Takakura & Kai 1966) provided a natural explanation of simple time profiles like that in figure 2 in terms of monotonic decay of the injected electrons but, when generalized to the case of a vibrating bottle (Brown 1973*a*, Brown & Hoyng 1975), can also produce highly structured time profiles such as in

figures 3 and 4. Burst variations occur principally through betatron acceleration of electrons in the varying trap field so that, as in the other models, continuous acceleration is involved but, subsequent to the initial injection, the mechanism is sufficiently simple to permit quantitative modelling and comparison with observations (see §3). The instantaneous spectrum $N(E, t)$ (electrons keV^{-1}) of all the trapped electrons is inferred from the X-ray flux (1) to be (Brown 1971, 1975)

$$N(E, t) = \frac{3.6 \times 10^{41}}{n(t)} f(\gamma) A E^{-\gamma+\frac{1}{2}}, \quad (4)$$

where $n(t)$ is the ambient plasma density, inhomogeneity effects being neglected here (cf. Brown 1972*b*, 1975).

3. OBSERVATIONAL EVIDENCE BETWEEN RIVAL BREMSSTRAHLUNG MODELS

As yet no test can be made of models (a) or (b) above, nor of the initial injection phase of model (c), in terms of theoretical forms for $\mathcal{F}(E, t)$ or $N(E, t)$ since the basic problem of dynamic dissipation remains unsolved (cf. summary by Kuperus in this volume). However, in the oscillatory phase of the electron trap model (figure 5*c*), the electron flux and spectrum are modulated by the betatron action of the varying trap field (Brown & Hoyng 1975) and, combined with variation in the ambient density n , result in the X-ray burst time profile. Though the actual flux and spectral variations with time depend on the unknown field variation $H(t)$, it is found that a correlation should exist between instantaneous values of γ and of the effective

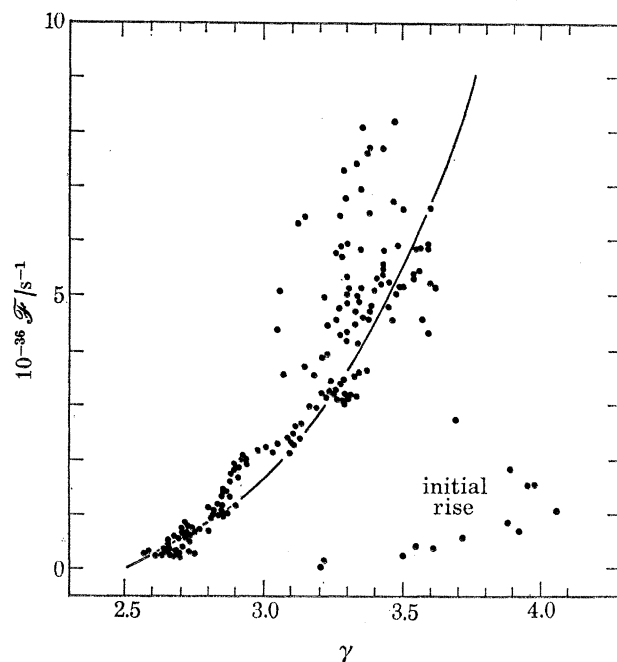


FIGURE 6. Observed correlation (Hoyng *et al.* 1975) between inferred instantaneous electron injection rates $\mathcal{F}(t)$ (electrons s^{-1}) above 25 keV and instantaneous X-ray spectral indices $\gamma(t)$ (cf. figure 7) during the event of 4 August 1972 (figure 4). The 'knee' of points in the bottom right was swept out during the rapid rise of the event (till 6:22:54 U.T.). The solid curve is the (\mathcal{F}, γ) correlation predicted by Brown & Hoyng (1975) for electrons driven by betatron action of an oscillating magnetic trap after initial acceleration by a large scale electric field with runaway above 15 keV.

electron flux \mathcal{F}_1 above any reference energy (chosen as 25 keV), the form of the correlation depending only on the initial electron energy/pitch-angle distribution function.

In the event of 4 August 1972 (figure 4) with count statistics adequate for accurate inference of $\mathcal{F}_1(t)$, $\gamma(t)$, Hoyng, Brown & van Beek (1975) found just such a correlation observationally and Brown & Hoyng (1975) have shown that the betatron model fits it well – see figure 6 – if initial electron injection is by direct electric field acceleration in a hot plasma at a few tens of megakelvins. The fit to the correlation data allows deduction of the approximate form

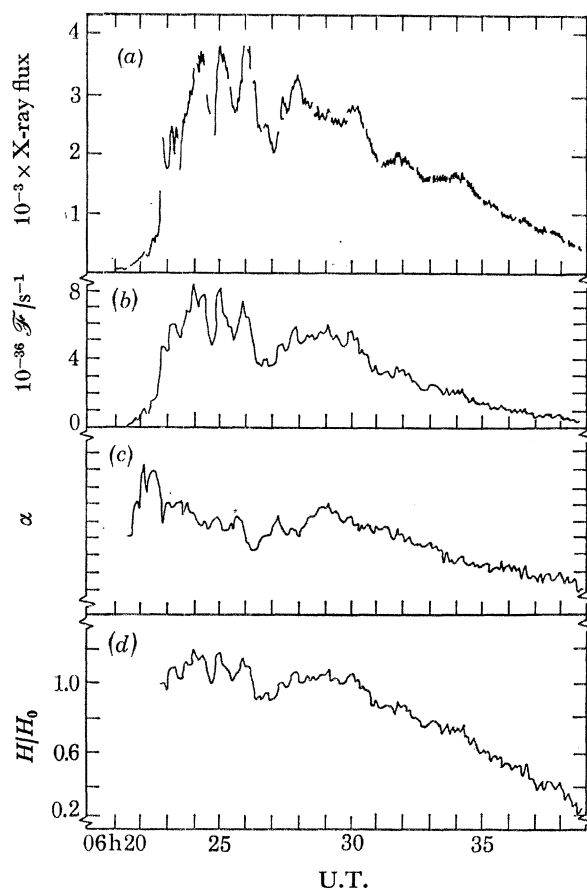


FIGURE 7. (a) First channel (29–41 keV) count rate for the 4 August 1972 event together with (b) inferred (thick target) electron injection rate \mathcal{F} above 25 keV and (c) the X-ray power-law index γ . Profile (d) shows the inferred magnetic field variations required in a magnetic trap (cf. figure 5c) subsequent to initial electron injection (when $H = H_0$) to produce the burst profile (Brown & Hoyng 1975). Note particularly how small an H/H_0 variation is needed to produce the major burst oscillations.

of $H(t)$ required in the trap vibration with the result shown in figure 7 together with $\mathcal{F}(t)$ and $\gamma(t)$. This analysis is essentially the first quantitative model of the time development of a hard X-ray burst and the good agreement with the data lends strong support to the concept of coronal trapping in large events (cf. Frost & Dennis 1971).

A second test of models in terms of acceleration characteristics has been suggested by Datlowe & Lin (1973). Comparison of (3) with (2) or (4) above shows that thick and thin

targets require a different electron flux spectral index δ at acceleration to yield the same bremsstrahlung index γ , namely,

$$\delta_{\text{thick}} = \gamma + 1, \quad (5)$$

$$\delta_{\text{thin}} = \gamma - 1 \quad (6)$$

(due to collisional hardening of the electron spectrum within the thick target source – Brown 1971, Syrovatskii & Shmeleva 1972). Datlowe & Lin (1973) showed that (6) was more nearly satisfied than (5) in one burst *if* the acceleration index δ can correctly be identified with the index of electrons found in interplanetary space (Lin 1974). The chief weaknesses in this argument lie firstly in the low escape probability ($< 1\%$) which has to be assigned to flare electrons to explain their observed scarcity – this makes them highly atypical – and secondly in the adoption of mean γ and δ values from their variation through the event.

Clearly the models in figure 4 differ above all in their spatial distribution and particle stream geometry so, though these cannot yet be directly resolved (cf. Brown, van Beek & McClymont 1975), a number of indirect arguments have been based on this distinction. Specifically the close synchronism of various flash phase phenomena, occurring at widely differing heights in the solar atmosphere, with hard X-ray features – e.g. the e.u.v. and microwave bursts (Parks & Winckler 1971) – has been invoked in support of various models. The rapidity with which 10^4 eV electrons traverse the solar atmosphere renders such observations inconclusive but the correspondence of hard X-rays with H α kernels both in time (Vorpahl 1973) and space (Takakura *et al.* 1971) seems indicative of a thick target.

Somewhat more direct information on the heights of sources has been obtained by Roy & Datlowe (1975) by identifying bursts with flare active regions behind the limb, thus setting lower (occultation) limits to source heights. The results are presented as a case against the thick target which is dominated by chromospheric emission. Brown & McClymont (1975) have, however, calculated the expected height distribution of thick target X-rays and shown that there is sufficient coronal component from this model to be compatible with Roy & Datlowe's (1975) data. Clearly both the thin target and electron trap models are consistent with behind-the-limb events but the former is only so at the expense of efficiency since the source electrons traverse the 'thin' coronal plasma once only (cf. equations (2) and (3)) dumping most of their energy uselessly in the high corona (Brown & McClymont 1975; Brown 1975).

Finally, models have been compared in terms of the anisotropy and polarisation of the bremsstrahlung from their differing electron stream geometries. Though detailed theoretical calculations are available for some models (Haug 1972; Brown 1972*a*, cf. Brown 1975) the situation has now been complicated by the recognized importance of the backscattering of primary source X-rays from the dense photosphere (Tomblin 1972; Santangelo, Horstman & Horstman-Moretti 1973). Polarization observations (Tindo *et al.* 1970, 1972*a, b*; Nakada *et al.* 1974) are likewise obscured by a combination of instrumental effects (Nakada *et al.* 1974), contamination of the calibration procedure by photospheric albedo photons (Brown, McClymont & McLean 1974) and the uncertain role of thermal emission in the observed energy range. Directivity studies from burst longitude distributions (Kane 1974; Datlowe, Hudson & Peterson 1974*b*) seem at best to set an upper limit of some 50% to the centre-limb variation, much less than predicted for simple models with no thermal or albedo component.

In retrospect it seems most likely that satisfactory distinction of model geometry must await the advent of hard X-ray imaging and improvement of the observations discussed here.

4. THE ELECTRON ACCELERATION PROBLEM

Irrespective of the model, observed X-ray burst characteristics do permit inference of several important general requirements of the electron acceleration mechanism. The most important of these findings are summarized here, being based largely on recent analysis of the E.S.R.O. TD-1A data by Hoyng *et al.* (1975).

(a) *Total energy and number of electrons*

It is not uncommon in the literature for acceleration mechanisms to be discussed in terms of type III electron requirements, e.g. according to Priest & Heyvaerts (1974), about 10^{29} – 10^{30} electrons above 30 keV. This trend apparently continues despite the steady increase in the estimated requirement for bremsstrahlung production of a hard X-ray burst, namely, more than 10^{39} electrons above 30 keV in a very large burst, i.e. *ten orders of magnitude more than a small type III*. Such results are based on integration of equations (2), (3) or (4) over the burst duration which has been done approximately by Kane (1974) and Lin (1974) for small events and rather accurately by Hoyng *et al.* (1975) for larger events. Since the spectra are always of roughly inverse power-law form (cf. §4*c* below) the greatest uncertainty lies in the low boundary energy E_1 adopted (Neupert 1968; Brown 1971; Syrovatskii & Shmeleva 1972) – the total electron numbers varying like $E_1^{-\delta+1}$ and their total energy like $E_1^{-\delta+2}$. Table 1 shows typical results for the total energy and numbers in medium and large events from Hoyng *et al.* (1975) based on a conservative upper limit to E_1 of 25 keV. Decreasing E_1 to 10 keV would increase the totals by one to two orders of magnitude.

Examination of these numbers shows the electron energy to be sufficient in many cases to supply all requirements in the thermal flare insofar as these are known. (Datlowe *et al.* 1974*a* claim there is more energy in the soft X-ray plasma but this is uncertain by 1–2 orders due to the unknown density there.) This has created a school of thought in which the bremsstrahlung electrons are the primary product of energy release in some flares and provide the mechanism for transfer of energy from the site of release to all parts of the thermal flare flash. The phenomenological evidence in support of this model and its conceptual simplicity have been reviewed and emphasized by Hudson (1973), Brown (1973*b, c*) and Smith (1974) while aspects of the physics of the heating have been widely considered (e.g. Švestka 1970; Najita & Orrall 1970; Korchak 1971; Strauss & Papaggianis 1971; Cheng 1972; Hudson 1972; Syrovatskii & Shmeleva 1972).

More recently, calculations of the electron-heated flare structure have become precise enough (Brown 1973*c*; Shmeleva & Syrovatskii 1973) to allow comparison with H α profiles (Canfield 1974) and with masses of flare ejecta (Brown 1973*c*) with promising results. The model is, however, still not adequately defined since there is still no consensus over the relative importance of collisional and conductive heating in the optical flare or over the ionisation balance there (Brown 1973*d, 1974a*; Somov & Syrovatskii 1974). Furthermore the neglect of a consistent radiative transfer treatment of the radiative losses in the optical flare (Canfield 1974) and of the hydrodynamic response of the atmosphere urgently require to be remedied.

Attractive as this model may be, the implications of table 1 for the primary process of particle acceleration cannot be stated too strongly. The figures for a large event represent the release of an energy equal to the total in the potential field calculated for a large active region into the form of over 10^{39} electrons – the number of electrons in a cubic solar radius of the

high corona or the entire number superincumbent on the optical flare (10^{19} cm^2) down to the depth where $n \simeq 10^{13} \text{ cm}^{-3}$. That is, the bremsstrahlung interpretation of X-ray bursts demands that the entire flare volume be considered in the supply of electrons. In view of the severity of this requirement, in §5 alternative X-ray source interpretations are considered.

TABLE 1. TYPICAL PARAMETERS OF ELECTRON ACCELERATION FROM BREMSSTRAHLUNG X-RAY BURST MODELS

	large event	moderate event
duration T/s	$10^2\text{--}2 \times 10^3$	20–200
periodicities/s	16–130	none?
shortest e -folding time scales τ_{min}/s	10	2
peak electron injection rate (above 25 keV) \mathcal{F}_{25}/s^{-1}	8×10^{36}	10^{36}
peak electron energy flow (above 25 keV) $\mathcal{P}_{25}/J \text{ s}^{-1}$	2×10^{22}	3×10^{21}
total electrons $\int_T \mathcal{F}_{25} dt$	3×10^{39}	3×10^{37}
total energy $\int_T \mathcal{P}_{25} dt/J$	2×10^{25}	2×10^{23}
X-ray spectral index γ	2.5–4.0	3.0–6.0

(b) *Time scales*

A number of times characterize a burst and hence the acceleration mechanism. Table 1 shows the typical durations T of medium and large events from Hoyng *et al.* (1975) while Kane (1974) and Datlowe *et al.* (1974a) have presented results for small events. These figures represent the total time over which electrons are accelerated in some way though this may be in two phases (Frost & Dennis 1971; Brown & Hoyng 1975). Note that intense events have by far the longest durations so that the high total energy injected is at least as much due to the duration as to the higher peak flux.

More important for acceleration mechanisms is the shortest time scale on which a typical peak flux is reached. Hoyng *et al.* (1975) have emphasised that the appropriate time for studying the energy dissipation rate is the e -folding time scale τ for change in the *total* burst count rate rather than the duration of small features superposed on the general flux. That is:

$$\tau = \frac{1}{d \lg I/dt} \simeq \frac{1}{2} \frac{(C_{i+1} + C_i)}{(C_{i+1} - C_i)} \Delta t, \quad (7)$$

where C_i is the instrumental count in the i th integration interval Δt . Furthermore, time profiles exhibit spurious rapid changes due to Poisson fluctuations in C . Generally these fluctuations ($\simeq \sqrt{C}$) render unreal any structure with an apparent time scale longer than

$$\tau_{\text{noise}} \simeq \frac{1}{2} \sqrt{C} \Delta t. \quad (8)$$

However, Hoyng *et al.* (1975) note that an individual $\tau \ll \frac{1}{2} \sqrt{C} \Delta t$ may still be a statistical fluctuation and emphasize that the presence of short-time scales can only be tested by comparing their frequency of occurrence with expectation from Poisson noise. Applying this approach to both the count time profile and to its Fourier power spectrum, Hoyng *et al.* find that burst e -folding time scales are never as short as the 1.2 s resolution of the TD1-A instrument but have the lower limits τ_{min} shown in table 1.

Burst periodicities have also been sought and apparently found in a few large events, either by inspection (Frost 1969) or by Fourier analysis (Parks & Winckler 1971), in the 10–30 s

range. In small events the count statistics are often too poor and the number of data points C_i in the time series too few for the Fourier spectrum to stand a chance of revealing periodicities above the Poisson and discretization noise. On the other hand the duration and statistics of the 4 August 1972 event (figure 4) were so favourable that Hoyng *et al.* (1975) were able to establish the statistical reality of 30, 60 and 120 s periods in the profile and to show these dying away in a dynamic Fourier analysis (Power–frequency–time plot). In addition these periods were also found to be present in both the inferred electron flux $\mathcal{F}(t)$ and in the spectral index $\gamma(t)$.

(c) *Acceleration spectra*

The various stages in conversion from observed pulse height distributions to electron spectra in a solar bremsstrahlung source have been dealt with by several authors. Hoyng & Stevens (1974) have developed a fast method for unfolding the best representation of the true photon spectrum, from pulse heights, through the instrumental response. Such analysis shows that a two parameter fit is the best that can be done in small bursts since photons are only detected in about four channels and that the single power-law (1) is a fair approximation. Larger events do reveal a real steepening of the spectrum above 60–100 keV (Frost 1969; van Beek, de Feiter & de Jager 1973) though the data do not indicate a *sharp* spectral break (Hoyng *et al.* 1975). Brown (1971, 1975) has considered the problems of inversion from photon spectra to effective electron spectra in the source both from the analytic and numerical viewpoints. These indicate that electron spectra cannot be well determined from bremsstrahlung data of finite accuracy and lead to the conclusion that any simple model of the spectrum – e.g. a single power law $\sim E^{-\delta}$ – is as good as can be done but that no specific model should be given special physical significance. This view is reinforced by the existence of several model dependent effects (directionality, source inhomogeneity, and the photospheric albedo) which can distort a basic power-law spectrum. The statistics of occurrence of spectral indices γ have been analysed by Kane (1974) and by Datlowe *et al.* (1974*a*) showing higher values of γ to be most frequent except in large bursts which are usually hard. Neither these results nor the diverse evolution of $\gamma(t)$ observed by these authors and by Hoyng *et al.* (1975) has, however, yet led to definitive physical interpretation with the exception of the ($\mathcal{F}(t)$, $\gamma(t)$) correlation shown in figure 6 and already discussed in §3.

Power-law fitting is generally based on data between 10 and 100 keV or so. Behaviour of the impulsive burst spectrum below 10 keV is totally obscured by the gradual (thermal?) component (figure 1) while at the high energy end 1 MeV is around the limit of detectability (Chupp *et al.* 1973). This is particularly awkward since it is in these two extremes that ways might be found out of the electron acceleration problem posed in §4, as discussed below.

5. POSSIBLE SOLUTIONS OF THE ELECTRON ENERGY AND NUMBER PROBLEM

If the acceleration of $\geq 10^{39}$ electrons ($\geq 10^{25}$ J) above 25 keV is too demanding, alternative burst interpretations to the models in §2 must be sought, which demand less of the acceleration mechanism. Directions in which it might prove profitable to look include the following.

(a) *'Recycling' of the electrons*

Hoyng *et al.* (1975) and Brown (1975) have suggested that the *number* of electrons N required for a burst could be greatly reduced if ϕN electrons ($\phi \ll 1$) could be confined in a region where

they were each repeatedly accelerated then decelerated $1/\phi$ times during the event. The difficulty lies in obtaining a region throughout which acceleration can occur *and* containing enough plasma to decelerate the electrons *collisionally* since, if collective losses are invoked to do this, the bremsstrahlung efficiency falls severely (Brown 1975). This mechanism would not in any case reduce the *total energy* supply needed unless in some obscure way the energy lost collisionally feeds back efficiently into the accelerating mechanism (e.g. by conversion to turbulence).

In connection with their betatron trap model, Brown & Hoyng (1975) have noted that most of the energy initially injected into the trapped electrons may be ultimately returned to the trapping active region field as the bottle expands, rather than collisionally dissipated.

(b) *The synchrotron and inverse Compton mechanisms*

Korchak (1967, 1971) has discussed the role of the synchrotron (s) and inverse Compton (i.C.) mechanisms in comparison to bremsstrahlung and concluded that, *a priori*, under average flare conditions, bremsstrahlung is the most probable but warns that each should be evaluated in any particular model. One common misconception is that the inverse Compton effect is non-negligible only at energies $\epsilon \lesssim 1$ keV which is swamped by thermal flare emission in any case. In fact the synchrotron and i.C. emission from a single power-law electron spectrum totally dominate at *high* energies over bremsstrahlung from the same spectrum (the photon indices being $\gamma_s = \gamma_{i.C.} = (\delta + 1)/2$ and $\gamma_b = \delta + \frac{1}{2}$ for electron index δ). Korchak's equations give

$$I_s(\epsilon) \simeq 3.5 \times 10^{-25} (26H/\epsilon)^{(\delta+1)/2} (1.6 \times 10^{-9})^{\delta-1} \mathcal{N}_1 E_1^{\delta-1} \quad (9)$$

and

$$I_{i.C.}(\epsilon) \simeq 9.0 \times 10^{-22} (7.9 \times 10^{-9})^{(\delta+1)/2} \mathcal{N}_1 E_1^{\delta-1} \quad (10)$$

as the synchrotron and i.C. X-ray fluxes (cf. (1)) from the electron spectrum $E^{-\delta}$ with \mathcal{N}_1 electrons above energy E_1 (thus $\mathcal{N}_1 E_1^{\delta-1}$ is independent of E_1), when the field is H gauss (10^{-4} T).

As an illustration, the event of figure 4 required, in the electron trap bremsstrahlung model (Brown & Hoyng 1975), $\mathcal{N}_1 \simeq 10^{39}$ for $E_1 = 25$ keV, $\delta = 3$ and $n \simeq 4 \times 10^7$ cm $^{-3}$, $H = 12$ G (1.2 mT), to fit the observed flux I_o , namely

$$I_b = I_o = 1.2 \times 10^7 \epsilon^{-3.5}.$$

From the relativistic extrapolation of this spectrum of particles (9) and (10), however, predict fluxes

$$\left. \begin{aligned} I_s &= 5.4 \times 10^4 \epsilon^{-2} \\ I_{i.C.} &= 3.5 \times 10^4 \epsilon^{-2} \end{aligned} \right\} \quad (11)$$

and

$$I_s/I_b = 4.5 \times 10^{-3} \epsilon^{1.5}. \quad (12)$$

Evidently the *synchrotron emission would dominate the bremsstrahlung at all energies above 36 keV* (with the i.C. contribution almost as great) and this in just a 12 G field!

The key questions in the relative roles of the three emission process are then whether the electron spectrum could theoretically extend to ultrarelativistic energies (some 10–100 MeV for i.C. emission and above a GeV for synchrotron X-rays, Korchak 1971) and, if it did, would it be compatible with other observational constraints. It has not yet been convincingly shown that the existence of an ultrarelativistic electron component, as the extension of a relatively small flux of sub-relativistic electrons with spectrum steepening at high energies, presents any more difficulties of compatibility with radio and interplanetary data than encountered

with conventional bremsstrahlung interpretations – these requiring much more energy supplied to the electrons. The extent of the reduction achieved in the necessary supply of electrons is seen by applying (9) to give the \mathcal{N}_1 (for several E_1) needed for the 4 August 1972 event, as shown in table 2 for a 1 mT field (electron spectrum $\sim E^{-6}$ in this energy range). Also shown are the electron lifetimes against synchrotron losses (Korchak 1971) which, considering the time structure of typical bursts (figures 2–4), pose no problems to this interpretation, contrary to Korchak (1971) and Svestka (1971). Evidently for E_1 significantly above 10^9 eV, \mathcal{N}_1 and the total energy \mathcal{E}_1 are trivially small in comparison to the bremsstrahlung model requirements (table 1).

TABLE 2. TOTAL NUMBER \mathcal{N}_1 AND TOTAL ENERGY \mathcal{E}_1 OF ELECTRONS ABOVE SEVERAL ENERGIES E_1 IN THE ULTRARELATIVISTIC SPECTRUM NEEDED TO PRODUCE THE LARGE EVENT OF FIGURE 4 BY SYNCHROTRON EMISSION. τ_s IS THE ELECTRON LIFETIME.

E_1/eV	\mathcal{N}_1	\mathcal{E}_1/J	τ_s/s
10^9	10^{26}	2×10^{26}	1800
10^{10}	10^{21}	2×10^{22}	180
10^{11}	10^{26}	2×10^{18}	18

(c) *The thermal contribution*

Chubb (1971) suggested that the power-law X-ray spectrum observed above 10 keV or so should not be taken as evidence against emission by the thermal flare plasma since, though locally Maxwellian, this may be far from isothermal. Brown (1974*b*) put this argument on a quantitative basis by showing that any X-ray spectrum $I(\epsilon)$ can be generated by a thermal plasma with differential emission measure $\phi(T)$ ($\text{cm}^{-3} \text{K}^{-1}$)

$$\phi(T) = \frac{1.4 \times 10^{45}}{T^{\frac{3}{2}}} \mathcal{L}^{-1} \left\{ I(\epsilon); \frac{1.16 \times 10^7}{T} \right\} \quad (13)$$

\mathcal{L}^{-1} being the inverse Laplace transform. The two commonest objections posed against this model in the literature are in fact mutually contradictory. On the one hand it is argued (e.g. Kahler 1971) that conduction down the steep temperature gradients implied by (13) would cause source cooling in times much shorter than typical event durations while, on the other, (e.g. discussion following Brown 1974*b*) it is objected that a thermal source could not vary rapidly enough to reproduce rapid burst variations! Conduction analysis based on (13) shows that the cooling times are entirely compatible with the burst time scales shown in table 1 (Brown 1974*b*). Thus, though it may be necessary to envisage a source with hot dense cores rather than the filamentary structures so far considered, thermal interpretation cannot be ruled out up to 40–100 keV.

The crucial point here is that the energy above which thermal gives way to non-thermal emission is critical for inferring the total non-thermal electron energy. Thus if thermal photons dominated to 50 rather than 20 keV, an E^{-5} electron spectrum would involve 94 % less energy and 97 % less electrons. For this reason the fullest possible understanding of the temperature structure of the thermal flare plasma is essential.

6. THERMAL X-RAYS

Reference back to figure 1 shows how a transition occurs at longer wavelengths from the impulsive spiky hard X-ray time profile, coincident with the optical flash, to the prolonged gradual soft X-ray profile which closely replicates the H α development. Extensive studies have been carried out on these soft bursts in terms of the statistics of their fluxes, rise and decay times, relation to H α and so forth (e.g. Hudson, Peterson & Schwartz 1969; Culhane & Phillips 1970; Thomas & Teske 1971; Drake 1971; Datlowe *et al.* 1974*b*) while very intimate knowledge has been gained of the numerous lines in their spectra (cf. Neupert 1969; Walker 1971; Culhane & Acton 1974; for example). What is still lacking is a real contribution to understanding the structure of the hot flare plasma itself. Thus many analyses (e.g. Datlowe *et al.* 1974*b*) are still carried out by ‘fitting’ an isothermal emission function (with the two parameters – temperature T and emission measure $\int_V n^2 dV$) to the observed spectrum, however many channels are actually incorporated in the instrument. Again, on the assumption of homogeneity, line measurements permit evaluation of element abundances and non-steady ionization equilibrium in the plasma.

Interesting as such analyses may be from the atomic physics viewpoint, isothermal models are scarcely likely to suffice for modelling energy flow in the hot flare plasma (cf. Herring & Craig 1973; Craig 1974). In particular, if the differential emission measure is $\phi(T)$ then:

- (i) the total thermal energy of the plasma is

$$\mathcal{E}_{\text{th}} \simeq 3 \int_T \frac{\phi(T)kT}{n} dT. \quad (14)$$

Thus if $\phi(T)$ is a steeply decreasing function of T , as may be the case (Craig 1974), most of \mathcal{E}_{th} resides at low T . Furthermore \mathcal{E}_{th} depends on the inferred plasma density n which is highly uncertain and itself dependent on the temperature structure model.

- (ii) The upper temperature limit of $\phi(T)$ is critical for inference of the *non-thermal* electron energy in the flare (see §5*c* above).

(iii) Cooling of the hot plasma is expected to be predominantly by conduction (e.g. Culhane, Vesecky & Phillips 1971) which depends critically on the source temperature structure (Brown 1974*b*; Craig 1974). This issue is crucial not only for the energy supply needed to the soft X-ray plasma itself but also for the effect of conduction on the underlying optical and u.v. flares (e.g. Švestka 1973; Brown 1974*a*; Somov & Syrovatskii 1974).

The need for a multi-temperature model was first emphasized by Herring & Craig (1973) who established the great improvement obtained by using a two-temperature structure. This has recently been incorporated by Herring (1974) into the first theoretical model of the plasma temperature structure.

Figure 8 shows the time evolution of a typical thermal burst (after Datlowe *et al.* 1974*b*) in terms of a fitted isothermal model, i.e. the parameters $\int n^2 dV$ and T . The surprising feature of the time development is that T starts decreasing well before the peak burst flux, the rise being governed by a continuing rise in the emission measure. Datlowe *et al.* (1974*b*) show correctly that this must be due to the ‘addition of new material’ (V increasing) to the hot plasma rather than to compression (n increasing) but claim that the mechanism involved cannot be conduction since T is decreasing – this latter argument being fallacious since based on a single isothermal region. Zaumen & Acton (1974) in fact show that only a conductive extension of

the hot region could model the $\int n^2 dV$ increase with decreasing T and present a simple two temperature model of the situation.

Attempts to find more detailed models of $\phi(T)$ than just two components have been made for both flares and active regions (e.g. Dere, Horan & Kreplin 1974, Batstone, Evans, Parkinson & Pounds 1971) but have run into problems of unphysical solutions ($\phi < 0$) unless a positive solution is forced (Batstone *et al.* 1970, cf. Parkinson, this volume). At first sight this is astonishing since the spectral resolution at long wavelengths ($\lesssim 0.1\%$) is more than two orders better than at high energies ($\sim 20\%$, van Beek 1973) where we can apparently obtain reasonable models of the source electron spectra for any adopted emission mechanism (§§ 2, 4 and 5 above). The explanation lies primarily in the fact that soft X-ray spectra (continuum or lines) are not temperature sensitive enough for the problem. This may be alternatively expressed (P. Hoyng, private communication) in terms of the numerical ill-conditioning of the inversion problem from the spectrum $F(\lambda)$ to the function $\phi(T)$. For either a series of n lines, or a series of n continuum measurements, at wavelengths λ_j , the problem reduces to solving

$$\sum_{i=1}^n G(\lambda_j, T_i) \Phi_i = F(\lambda_j), \quad (15)$$

where the Φ_i are a set of effective partial emission measures centred about a set of n representational temperatures T_i , a slow temperature ($T^{\frac{1}{2}}$) dependence being absorbed in Φ from G . Then the kernel matrix G – the emission function – is dominated by the dependence

$$\sim \exp(-C/\lambda_j T_i)$$

which is of severely ill-conditioned form.

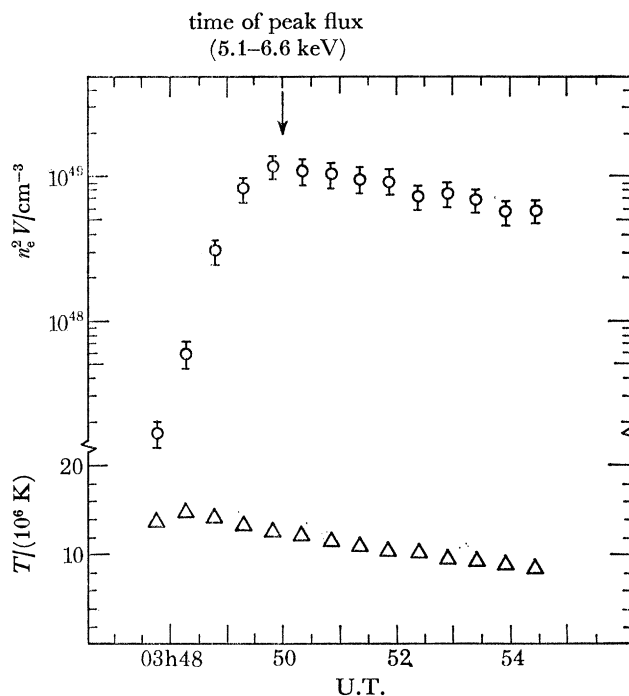


FIGURE 8. Time evolution of isothermal model parameters – temperature $T(K)$ and emission measure $n^2 V(\text{cm}^{-3})$ – fitted to the event of 26 January 1972 by Datlowe *et al.* (1974*b*). The time of the peak flux in the 5.1–6.6 keV data is also shown. Note that T declines through most of the event.

This ill-conditioning has the effect of greatly magnifying fractional errors in F_j (due to count statistics and calibration) to result in large relative errors in the solution Φ_i , the typical maximum error magnification being measured by the condition number η of matrix G . η depends on the instrumental choice of λ_j and on the selected T_i representation but a typical (spectrum line) case is that of Batstone *et al.* (1971) in their active region analysis. Brown & Craig (unpublished) find η to be around 50 for the Batstone matrix. Thus for a 5-temperature source analysis based on five resonance lines, the data F_j would have to be better than 1% to guarantee a single significant figure in Φ_i . This precision demands that, considering the Poisson counting error $\sqrt{N}/N = 1/\sqrt{N}$ alone, the typical count should be $\simeq 10^4$ which is in practice virtually unattainable. Batstone *et al.* (1971) recorded only about 50 photons per line with a Poisson uncertainty of some 15%. Thus not a single figure of such a Φ analysis need be meaningful – hence the problem of negative emission measures arising in the attempt. Large increase of N through large areas or integration times are unlikely to help since the calibration errors remain large.

It must be emphasized that increasing n , by resolving more and more lines or using more and more pulse height discriminator levels in the continuum, *over a fixed total wavelength band*, merely makes matters worse in terms of solutions for $\Phi(T)$. This is tantamount to trying to improve the solution of two equations by introducing a third equation ‘between’ them. Clearly this can only increase the linear dependence of the matrix rows (since $\exp(-C/\lambda T)$ is monotonic in both λ and T) which is a major factor in producing ill-conditioning. Analysis of a simplified case (Brown & Craig) shows that η increases with n (λ_1, λ_n fixed) at least as fast as n^2 for large n due to the linear dependence alone (neglecting the matrix scaling which worsens the effect).

The least recognized but most important feature of all in this problem is that the reverse can occur. That is, on resubstitution of a spurious numerical solution Φ into (15), a small residual relative to the observed F may be found and the solution accepted on the grounds of consistency. What it means in practice is that, since a small change in F can result in a large change in Φ , a wide range of models Φ will ‘fit’ the data F equally ‘well’. To that extent the solution found may be regarded as being as good as one can get but, since such widely different solutions would be as ‘good’, the solution is of little physical value. This situation is well known in numerical analysis – e.g. ‘A characteristic feature of ill-conditioned equations is that a set of values for the unknown may be found which differs considerably from the solution of the equations but may, nevertheless, give small residuals for all the equations. For example . . . in this case values of residuals which are less than 1/2000 of the data still do not guarantee the accuracy even of the first figure in the x 's.’ (Hartree 1952.)

In conclusion, soft X-ray data at present fall between two stools. Bragg crystal spectrometry allows fairly accurate definition of some mean temperature over the source as a whole but not its distribution. Grazing incidence images with filtering (Vaiana *et al.* 1974) on the other hand clearly portrays the distribution of generally hot material but without much precision as to how hot. It appears most likely therefore that the spatial distribution of temperature in the flare, and the key problems associated with it, will only be resolved by combining high spatial with *moderate* spectral resolution in future experiments.

I am grateful to the Royal Society for the invitation to present this paper and for the provision of funds for my attendance.

REFERENCES (Brown)

- Arnoldy, R. L., Kane, S. R. & Winckler, J. R. 1968 *Astrophys. J.* **151**, 711.
- Batstone, R. M., Evans, K., Parkinson, J. H. & Pounds, K. A. 1970 *Solar Phys.* **13**, 389.
- van Beek, H. F. 1973 Ph.D. thesis, University of Utrecht.
- van Beek, H. F., de Feiter, L. D. & de Jager, C. 1973 To appear in *Proc. Eslab Symp.* (Saulgau 1973).
- Brown, J. C. 1971 *Solar Phys.* **18**, 489.
- Brown, J. C. 1972 *a Solar Phys.* **26**, 441.
- Brown, J. C. 1972 *b Solar Phys.* **25**, 158.
- Brown, J. C. 1973 *a Solar Phys.* **32**, 227.
- Brown, J. C. 1973 *b Proc. Leningrad Symp. on Solar Cosmic Rays*, June 1973.
- Brown, J. C. 1973 *c Solar Phys.* **31**, 143.
- Brown, J. C. 1973 *d Solar Phys.* **28**, 151.
- Brown, J. C. 1974 *a Solar Phys.* **36**, 371.
- Brown, J. C. 1974 *b In Coronal disturbances* (ed. G. Newkirk). Proc. I.A.U. Symp, 57, Surfer's Paradise, September 1973.
- Brown, J. C., McClymont, A. N. & McLean, I. S. 1974 *Nature, Lond.* **247**, 448.
- Brown, J. C. 1975 In *Solar γ -, X- and EUV-radiation* (ed. S. R. Kane). Proc. I.A.U. Symp. 68, Buenos Aires, June 1974.
- Brown, J. C. & McClymont, A. N. 1975 *Solar Phys.* **41**, 135.
- Brown, J. C., van Beek, H. F. & McClymont, A. N. 1975 *Astron. Astrophys.* **41**, 395.
- Brown, J. C. & Hoyng, P. 1975 *Astrophys. J.* **200**, 734.
- Canfield, R. C. 1974 *Solar Phys.* **34**, 339.
- Cheng, C. C. 1972 *Solar Phys.* **22**, 178.
- Chubb, T. A. 1971 In *Proc. Leningrad Symp. Sol. Terrest. Phys.*, vol. 1 (ed. Dyer).
- Chupp, E. L., Forrest, D. J., Higbie, P. R., Suri, A. N., Tsai, C. & Dunphy, P. P. 1973 *Nature, Lond.* **241**, 333.
- Craig, I. J. D. 1974 Ph.D. thesis, University College London.
- Culhane, J. L. & Phillips, K. J. H. 1970 *Solar Phys.* **11**, 117.
- Culhane, J. L., Vesecky, J. F. & Phillips, K. J. H. 1971 *Solar Phys.* **15**, 394.
- Culhane, J. L. & Acton, L. W. 1974 *Ann. Rev. Astron. Astrophys.* **12**, 359.
- Datlowe, D. W. & Lin, R. P. 1973 *Solar Phys.* **32**, 459.
- Datlowe, D. W. Elcan, M. J. & Hudson, H. W. 1974 *a Solar Phys.* **39**, 155.
- Datlowe, D. W., Hudson, H. S. & Peterson, L. E. 1974 *b Solar Phys.* **35**, 193.
- Datlowe, D. W. 1975 In *Solar γ -, X- and EUV-radiation* (ed. S. R. Kane). Proc. I.A.U. Symp. 68, Buenos Aires, June 1974.
- Dere, K. P., Horan, D. M. & Kreplin, R. W. 1974 *Solar Phys.* **36**, 459.
- Drake, J. F. 1971 *Solar Phys.* **16**, 152.
- Frost, K. J. 1969 *Astrophys. J.* **158**, L159.
- Frost, K. J. & Dennis, B. R. 1971 *Astrophys. J.* **165**, 655.
- Hartree, D. R. 1952 *Numerical analysis*. Oxford: Clarendon Press.
- Haug, E. 1972 *Solar Phys.* **25**, 425.
- Herring, J. F. & Craig, I. J. D. 1973 *Solar Phys.* **28**, 169.
- Herring, J. F. 1974 *Solar Phys.* **39**, 175.
- Hoyng, P. & Stevens, G. A. 1974 *Astrophys. Space Sci.* **27**, 307.
- Hoyng, P., Brown, J. C. & van Beek, H. F. 1975 (Submitted to *Solar Phys.*)
- Hudson, H. S. 1972 *Solar Phys.* **24**, 414.
- Hudson, H. S. 1973 In *High energy phenomena on the Sun* (ed. R. Ramaty & R. G. Stone). Proc. Goddard Symp. NASA. X-693-73-193.
- Hudson, H. S., Peterson, L. E. & Schwartz, D. A. 1969 *Astrophys. J.* **157**, 389.
- Kahler, S. W. 1971 *Astrophys. J.* **164**, 365.
- Kane, S. R. 1974 In *Coronal disturbances* (ed. G. A. Newkirk). Proc. I.A.U. Symp. 57, Surfer's Paradise, September 1973.
- Korchak, A. A. 1967 *Soviet Astron. A. J.* **11**, 258.
- Korchak, A. A. 1971 *Solar Phys.* **18**, 284.
- Lin, R. P. 1974 *Space Sci. Rev.* **16**, 184.
- McKenzie, D. L., Datlowe, D. W. & Peterson, L. E. 1973 *Solar Phys.* **28**, 175.
- Najita, K. & Orrall, F. Q. 1970 *Solar Phys.* **3**, 282.
- Nakada, M. P., Thomas, R. J. & Neupert, W. M. 1974 *Solar Phys.* **37**, 429.
- Neupert, W. M. 1968 *Astrophys. J.* **153**, L59.
- Neupert, W. M. 1969 *Ann. Rev. Astron. Astrophys.* **7**, 121.
- Parks, G. K. & Winkler, J. R. 1971 *Solar Phys.* **16**, 186.
- Petrosian, V. A. 1973 *Solar Phys.* **186**, 291.

- Priest, E. R. & Heyvaerts, J. 1974 *Solar Phys.* **36**, 433.
- Roy, J.-R. & Datlowe, D. W. 1975 *Solar Phys.* **40**, 165.
- Santangelo, N., Horstman, H. & Horstman-Moretti, E. 1973 *Solar Phys.* **29**, 143.
- Shmeleva, O. P. & Syrovatskii, S. I. 1973 *Solar Phys.* **33**, 341.
- Smith, D. F. 1974 In *Coronal disturbances* (ed. G. A. Newkirk). Proc. I.A.U. Symp. 57, Surfer's Paradise, September 1973.
- Somov, B. V. & Syrovatskii, S. I. 1974 *Solar Phys.* **39**, 415.
- Strauss, F. M. & Papaggianis, M. D. 1974 *Astrophys. J.* **164**, 369.
- Sweet, P. A. 1969 *Ann. Rev. Astron. Astrophys.* **7**, 149.
- Švestka, Z. 1970 *Solar Phys.* **13**, 471.
- Švestka, Z. 1973 *Solar Phys.* **31**, 389.
- Syrovatskii, S. I. & Shmeleva, O. P. 1972 *Soviet Astron. A. J.* **16**, 273.
- Takakura, T. & Kai, K. 1966 *Pub. Astron. Soc. Japan* **18**, 57.
- Takakura, T. 1972 *Solar Phys.* **26**, 151.
- Takakura, T., Ohki, K., Shilwya, N., Fujii, M., Matsuoka, M., Miyamoto, S., Nishimura, J., Oda, M., Ogawara, Y. & Ota, S. 1971 *Solar Phys.* **16**, 454.
- Thomas, R. J. & Teske, R. G. 1970 *Solar Phys.* **16**, 431.
- Tindo, I. P., Ivanov, V. D., Mandelshtam, S. L. & Shuryghin, A. I. 1970 *Solar Phys.* **14**, 204.
- Tindo, I. P., Ivanov, V. D., Mandelshtam, S. L. & Shuryghin, A. I. 1972a *Solar Phys.* **24**, 429.
- Tindo, I. P., Ivanov, V. D., Valnicek, B. & Livshits, M. A. 1972b *Solar Phys.* **27**, 426.
- Tindo, I. P., Mandelshtam, S. L. & Shuryghin, A. I. 1973 *Solar Phys.* **32**, 469.
- Tomblin, F. F. 1972 *Astrophys. J.* **171**, 377.
- Vaiana, G. S., Davis, J. M., Giacconi, R., Krieger, A. S., Silk, J. K., Timothy, A. F. & Zombeck, M. 1973 *Astrophys. J.* **185**, 447.
- Vorpahl, J. A. 1973 *Solar Phys.* **28**, 115.
- Walker, A. B. C. 1972 *Space Sci. Rev.* **13**, 672.